ISET Journal of Earthquake Technology, Paper No. 391, Vol. 36, No. 1, March 1999, pp. 61-71

RELATIONSHIP BETWEEN TEMPERATURE RISE AND NONLINEARITY OF A VISCOELASTIC DAMPER

M.L. Lai*, K. Kasai** and K.C. Chang***

*Abrasive Lab., 3M Company, Building 251-3B-13, St Paul, MN 55144, USA
**Structural Engineering Research Center, Tokyo Institute of Technology, Yokohama, Japan
***Department of Civil Engineering, National Taiwan University, Taipei, Taiwan

ABSTRACT

To our knowledge, this is the first systematic experimental and analytical work conducted to verify that the temperature rise in an acrylic-based viscoelastic material (VEM) may be the main source of non-linearity when the VEM is subjected to large shear strains up to 125%. A simple relationship between the temperature rise and the specific heat as well as strain energy of the VEM is proposed and verified experimentally. The finding of the temperature rise effects is important in two folds. First, the permanent material deterioration is not the main source of the non-linear material behavior as many researchers would think otherwise. In fact, the temperature rise effect on the material properties is temporary since experiments showed that the material returned to its original properties as the heat in the material was dissipated. Second, since the source of non-linearity is identified, a simple modification on many existing linear viscoelastic theories that work for small strains may be made to include the modeling of the VEM subject to large strains. A fractional derivative viscoelastic model is employed in this study, although any other appropriate linear VEM models may also be used. Findings in this work may be used to standardize the characterization of the VEM properties at large strains. The modified linear viscoelastic models may also be used in the damper design and analysis process to capture the underlying behavior of viscoelastic dampers that undergo large strain deformations.

KEYWORDS: Viscoelastic Damper, Nonlinear, Energy Dissipation Device, Fractional Derivative

INTRODUCTION

Viscoelastic dampers consisting of viscoelastic material (VEM) slabs bonded to steel plates have been tested in many laboratories in the United States, Japan and Taiwan and installed in 10 large buildings structures to reduce seismic and wind responses (Nielsen et al., 1994; Kaniktar et al., 1998; Miranda et al., 1998). It is known that the VEM properties vary with the ambient temperature and loading frequency. Consequently, the viscoelastic damper is designed to operate at the ambient temperature and fundamental frequencies of the structure (Chang et al., 1995). In addition, it has been recognized that the VEM exhibits an *apparent* nonlinear behavior when it is subjected to large strain loading (Chang et al., 1998). A linearization technique such as time-averaged treatment is usually used to calculate the VEM shear moduli that represent the mechanical property of the VEM. The VEM moduli calculated in this manner decrease as the strain increases. Since the loading strain in the VEM varies in time, especially for seismic loading, a common question that arises for the designer is what VEM modulus value and which strain level should they use for design and analysis? In addition, there is no standardized linearization method in calculating the large strain VEM moduli.

This study indicates that in an acrylic-based VEM designated as 3M Brand ISD 110 (Lai et al., 1998), most of the *apparent* non-linearity can be accounted for by the temperature rise, which results from heat generation in the VEM during dynamic loading. It is then proposed that the VEM in a large range of strain can be characterized in a meaningful way by using small strain data that are linear along with a proper compensation of the temperature rise effects. This finding is important since it can greatly simplify VEM characterization as well as the damper design and analysis procedure for structures.

LINEAR VISCOELASTIC THEORY FOR SMALL STRAINS

When a VEM is under a sinusoidal shear stress $\tau(t)$ with a frequency ω, the shear strain $\gamma(t)$ will lag behind the stress by a phase angle δ as:

$$\tau(t) = \tau_o \sin(\omega t) \text{ and } \gamma(t) = \gamma_o \sin(\omega t - \delta) \tag{1}$$

where τ_0 and γ_0 are the stress and strain amplitudes, respectively. If the strain is plotted against stress, one will obtain an elliptical hysteresis loop.

Viscoelastic material is often characterized by storage, G', and loss, G'', shear moduli to represent the elastic and viscous properties respectively (Lai, 1995). The ratio of the loss to storage modulus is the loss factor, η, or so-called tangent delta $(\tan\delta)$ which is used along with G' to describe the material:

$$\eta = \frac{G''}{G'} = \tan\delta \tag{2}$$

G and G'' are related to the stress and strain amplitudes:

$$G' = \frac{\tau_o}{\gamma_o}\cos\delta \quad \text{and} \quad G'' = \frac{\tau_o}{\gamma_o}\sin\delta \tag{3}$$

From Equations (1) and (3), the stress-strain relationship becomes (Kasai et al., 1993)

$$\tau(t) = G'\gamma(t) \pm G''(\gamma_o^2 - \gamma^2(t))^{1/2} \tag{4}$$

which is an ellipse.

It is convenient to use complex variables to describe the VEM as

$$G^* = G' + jG'' \quad \text{and} \quad |G^*| = \frac{\tau_o}{\gamma_o} = (G'^2 + G''^2)^{1/2} \tag{5}$$

where $j = \sqrt{-1}$.

In structural and building applications, a viscoelastic (VE) damper typically consists of VEM slabs sandwiched between relatively rigid steel plates. The damper configuration is very simple and its operation is straightforward.

The VE damper can be characterized by the storage, K', and loss, K'', stiffness and are related to G' and G'' as

$$K' = \frac{G'A}{h}, \; K'' = \frac{G''A}{h} \quad \text{and} \quad \eta = \frac{K''}{K'} \tag{6}$$

where A is the total shear area and h is the thickness of the VEM slab. An important advantage of using the VE damper is that the damper is linearly scaleable as shown in Equation (6). The property of a large damper can be linearly predicted by testing a much smaller damper as long as the testing strain, temperature and frequency are kept the same. K'' can be further related to the viscous damping constant as

$$c = \frac{K''}{\omega} = \eta\frac{K'}{\omega} \tag{7}$$

where ω is the damper operating frequency.

OBSERVATIONS OF NONLINEAR BEHAVIOR AT LARGE STRAINS

Figure 1 shows shear stress against time for the 3M Brand ISD110 VEM deformed sinusoidally at 12.5%, 25%, 50% and 100% constant strain amplitudes, 23 °C ambient temperature and 1 Hz.

Two observations can be made. First, the performance of the VEM is essentially linear as is indicated by the test that among the four curves, the peak stress in the first cycle is almost linearly proportional to the strain amplitude. Second, the material is time-varying as demonstrated by the peak stress in each curve decaying in time, especially for large strain tests. The decay rate was different for each strain amplitude. Therefore the material is *apparently* nonlinear under the test conditions when a time-averaged approach is used to calculate the shear moduli for each strain amplitude. This decay in stress may solely be due to temperature rise in the VEM. This decay is not due to the deterioration of the material because the same decay curve can be reproduced after the VEM cools down to the initial temperature.

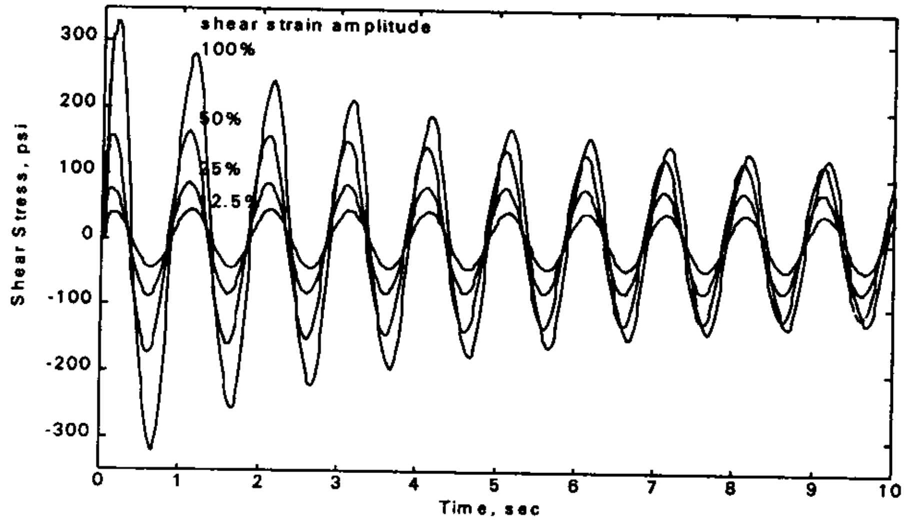

Fig. 1 Damper shear stress at 23°C ambient temperature, 1 Hz and various shear strain amplitudes (1 psi = 6.89 kPa)

SOURCE OF NONLINEARITY

When the VEM is subjected to a large strain excitation, a portion of the mechanical energy is dissipated and converted into heat, the temperature in the VEM rises as the by-product and the VEM softens. If the temperature rise in the VEM can be "turned off" and the shear stress is proportional to the shear strain with no decay in stress with time, then the VEM is *essentially* linear. Unfortunately, it is physically impossible to "turn off" the temperature rise in the VEM during a test.

An indirect test method is proposed as follows: an accurate linear VEM constitutive model verified by tests is constructed to represent the VEM properties at a small strain and various loading frequencies and ambient temperatures without considering the temperature rise effect. During a large strain loading, however, the temperature rise in the VEM is then "turned on" analytically in the *linear* VEM constitutive model. This model is used to predict the stress and strain time history of a test. If the correlation between the prediction and experiment is good, then one may conclude that the non-linearity effect is mainly from the temperature rise because the temperature rise in the VEM is the only parameter added to the linear model.

1. VEM Constitutive Model

Several VEM constitutive models have been proposed (Koh and Kelly, 1990; Kasai et al., 1993; Tsai, 1993 and 1994; Shen and Soong, 1995). Advantages of the fractional derivative rule as opposed to the more conventional integer derivative rule are the ability to accurately model the VEM over a large range of frequency with a small number of constants. The general form of fractional derivative model can be traced back to Gemant (1936). The simplified fractional derivative model developed by Kasai et al. (1993) has been found to be adequate and used in this study as

$$\tau(t) + aD^{\alpha}\tau(t) = G\left[\gamma(t) + bD^{\alpha}\gamma(t)\right] \tag{8}$$

where a, b, α and G are the constants to be determined from tests at small strains and t represents the time. D^{α} is fractional derivative operator (Kasai et al., 1993). Among the four constants, a and b are functions of temperature. Numerical integration is used to evaluate the stress-strain values as:

$$\tau^{(n)} + \frac{a}{(\Delta t)^{\alpha}} \sum_{j=0}^{N} w^{(j)} \tau^{(n-N+j)} = G\left[\gamma^{(n)} \frac{b}{(\Delta t)^{\alpha}} \sum_{j=0}^{N} w^{(j)} \tau^{(n-N+j)} \right] \tag{9}$$

where $w^{(0)} = \left[(N-1)^{1-\alpha} - N^{1-\alpha} + (1-\alpha)N^{-\alpha}\right] / \Gamma(2-\alpha)$

$w^{(n-j)} = \left[(j-1)^{1-\alpha} - 2j^{1-\alpha} + (j+1)^{1-\alpha}\right] / \Gamma(2-\alpha),\ for\ (1 \le j \le n-1)$

$w^{(n)} = 1/\Gamma(2-\alpha)$ and Δt is the time-step size. Equation (9) is used to solve for $\tau^{(n)}$ for a given γ^{n}.

The method of reduced variable or so-called viscoelastic corresponding states used by polymer chemists (Ferry, 1980) is employed to relate the $G'(\omega)$ values at a temperature T to that at a reference temperature T_{ref} as:

$$G'(\omega)\big|_{T_{ref}} = G'(c_s\omega)\big|_{T} \tag{10}$$

where $c_T(T)$ is the shifting factor and is a function of temperature. A shifting factor shown by Ferry (1980) is used here

$$c_s = e^{-p_1(T-T_{ref})/(p_2+T-T_{ref})} \tag{11}$$

where p_1 and p_2 are constants depending on a specific VEM.

The constants a and b are then related to the values at the reference temperature as

$$a = a_{ref} c_s^{\alpha} \text{ and } b = b_{ref} c_s^{\alpha} \tag{12}$$

Now, all constants, α, G, p_1, p_2, a_{ref} and b_{ref} are constants independent of frequency and temperature for a specific reference temperature. The constants for the acrylic-based VEM designated as 3M Brand ISD 110 used in this study at 24 °C are shown in Table 1. The units for stress is *psi* (1 psi = 6.89 kPa) and for temperature is °C. The procedure of determining these constants is discussed in the following section.

Table 1: Constants Used in the Model

α	G	p_1	p_2	a_{ref}	b_{ref}
0.6618	18.4064	17.8755	88.5055	0.0213	5.7601

The storage shear modulus, G', and loss factor, η can be written as (Kasai et al., 1993):

$$G' = G\frac{[1+b\omega^{\alpha}\cos(\alpha\pi/2)][1+a\omega^{\alpha}\cos(\alpha\pi/2)] + [ab\omega^{2\alpha}\sin^2(\alpha\pi/2)]}{[1+a\omega^{\alpha}\cos(\alpha\pi/2)]^2 + [a\omega^{\alpha}\sin(\alpha\pi/2)]^2} \tag{13}$$

$$\eta = \frac{[-a+b]\omega^{\alpha}\sin(\alpha\pi/2)}{1+[a+b]\omega^{\alpha}\cos(\alpha\pi/2)+ab\omega^{2\alpha}} \tag{14}$$

Figure 2 shows good correlation of the storage modulus, G', and loss factor, η, between the model and experimental data at 5% shear strain and 15°C, 24°C and 32°C ambient temperatures.

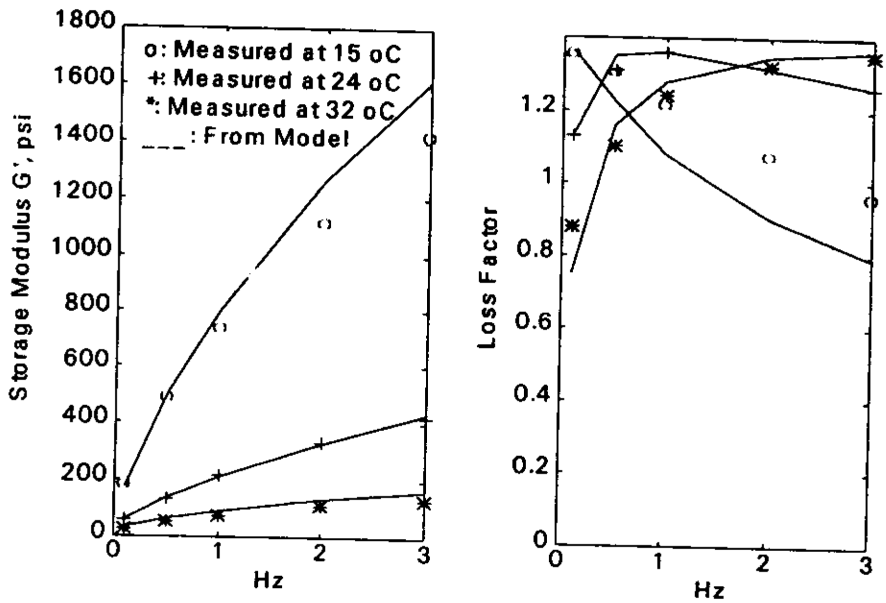

Fig. 2 Correlation of storage modulus and loss factor between data calculated from the model and those experimentally measured at 5% strain (1 psi = 6.89 kPa)

DETERMINATION OF CONSTANTS FOR THE FRACTIONAL DERIVATIVE MODEL

First, constants a_{ref}, b_{ref} and α were determined by fitting the experimental loss factor η values at the reference temperature of 24°C and a range of frequency from 0.1 to 3 Hz to Equation (14) in the least-square sense. The software used to conduct the least-square curve fitting was Matlab v. 5.2 by MathWorks Inc. Second, constant G was obtained by fitting the experimental G' values to Equation (13). Third, before constants p_1 and p_2 could be obtained, the shifting factor c_s was first sought. This was done by plotting G' in a range of frequency from 0.1 to 3 Hz at each VEM temperature against the reduced frequency $c_s f$ in a log-log scale as shown in Figure 3 where f is frequency. The temperatures used ranged from 15°C to 60°C and eleven different temperatures were employed. Through the trial-and-error process, c_s values at different temperatures were chosen until all data points relatively fell in one line according to the reduced-variable approach. c_s equals to one at 24°C because it was the reference temperature. The least-square technique was employed again to obtain in p_1 and p_2 Equation (11). The curve-fit is shown in Figure 4.

TEMPERATURE RISE IN A SHORT PERIOD OF TIME AND SPECIFIC HEAT

The fractional derivative model is then used to predict the VEM properties up to a 125% strain by including the temperature rise. The temperature in the VEM is updated using the shear stress, strain, density, ρ, and specific heat, s, of the VEM as:

$$T(t) = T_0 + \frac{1}{s\rho}\int_0^t \tau \, d\gamma \tag{15}$$

where T_0 is the initial temperature. In Equation (15), it is assumed that the heat generated in the VEM is all contained in the VEM and heat loss due to heat conduction is ignored. This assumption applies to the VEM studied since the external loading time to the VEM was short and the thermal conductivity of the VEM was small (0.00043 cal/cm.sec.°C).

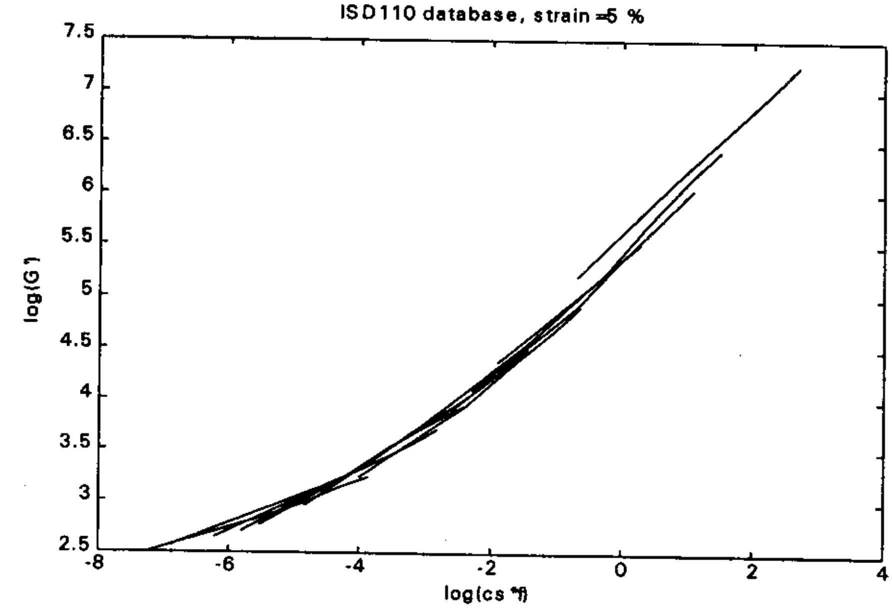

Fig. 3 log(G') at 0.1-3 Hz and different temperatures from 15 to 60°C versus log($c_s f$)

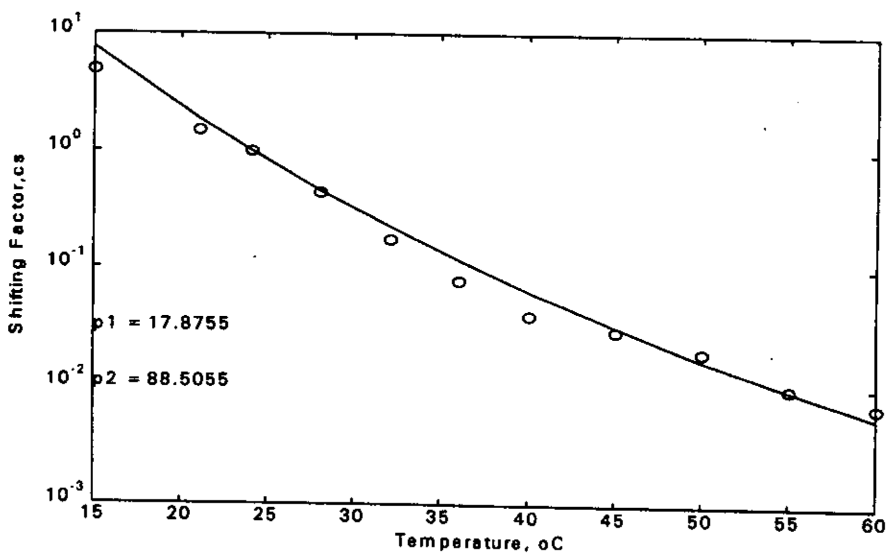

Fig. 4 Curve-fit of the shifting factor

CORRELATION BETWEEN TEST AND PREDICTION

1. Test Set-Up

Cyclic and ramp tests were conducted to verify the predicted results. Figure 5 shows the test set-up. MTS dynamic material testing machine was employed to conduct all tests. The upper end of the damper was bolted to the load cell of 1363 kgf (3000 lb) capacity. The lower end of the damper was attached to the hydraulic-driven actuator that was programmed to oscillate up and down. The two VEM slabs experienced mostly shear deformation when the actuator moved. A temperature-controlled chamber was used for changing the ambient as well as the initial damper temperatures. The damper temperature was considered stable, and test was initiated when the damper temperature and the ambient temperature were within 0.2°C. Force and displacement in each test were recorded simultaneously by a 4-channel Nicolett high speed data acquisition system. Fine thermocouples (T.C.) with response time constant less than 0.1 sec were used to record the ambient temperature and temperature in the VEM. The shear area of the VEM was 28.6 cm^2 (4.44 $inch^2$) and thickness was 1.27 cm (0.5 inch). The VEM specific heat was separately measured to be 0.45 cal/gm.°C and the density was 1.04 $gm./cm^3$.

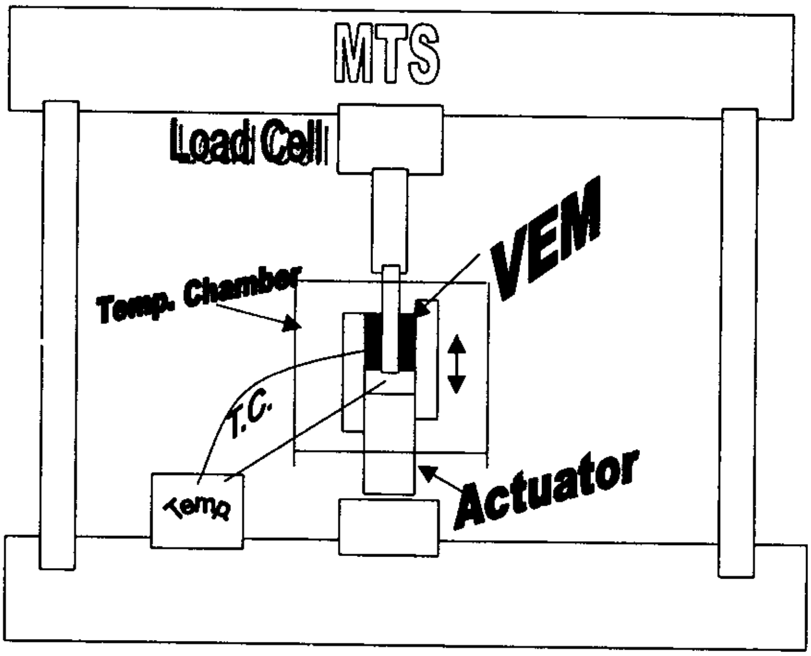

Fig. 5 Test set-up

2. Cyclic Test

Cyclic tests were conducted at various strain amplitudes, loading frequencies and ambient temperatures as shown in Figures 6(a)-6(h). The solid lines represent measured stresses and temperatures. The dashed lines represent the analytical results using the aforementioned fractional derivative model with the initial temperature and strain time history as inputs. Although 20 cycles in each test were recorded, only 10 cycles are shown here for clarity.

Testing under the wide strain (12.5% to 125%), frequency (0.5 Hz to 4.3 Hz) and temperature (22.5°C to 32°C) ranges, correlations between the experimental stress as well as VEM temperature and the analytical results were quite good. For large strain and high frequency tests, the stresses measured from the experiments were usually higher than the analytical results in the latter part of the cycles. This might be due to conduction of a small amount of heat from the VEM into the steel plates during the cycling and the overall VEM became slightly more rigid than was predicted assuming no heat loss from the VEM to the surrounding. Since the computation of the heat conduction for different damper geometry is quite involved, the proposed approach is simple and very useful for short duration excitations such as earthquakes. However, when considering long excitations such as those produced by wind, the heat conduction becomes dominant and should be considered fully.

When the temperature rise was "turned off" analytically, the stress became a constant amplitude and proportional to the strain for a fixed frequency and temperature. The VEM is then *essentially* linear.

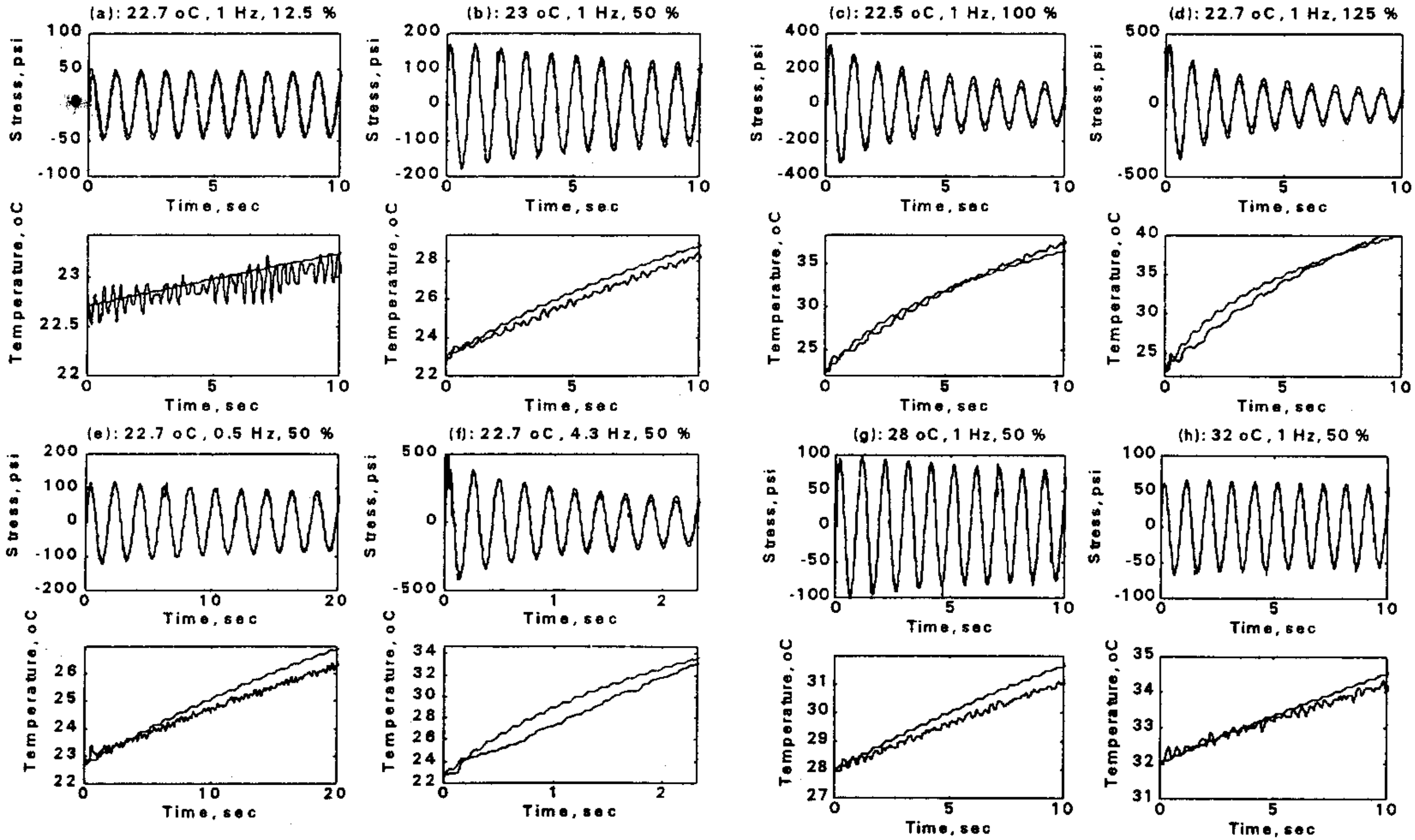

Fig. 6 Measured (solid line) and analytical (dashed line) stress (1 psi = 6.89 kPa) and VEM temperature versus time.

(a) for 1 Hz, 22.7°C initial temperature and 12.5 % strain	(b) for 1 Hz, 23°C initial temperature and 50 % strain	(c) for 1 Hz, 22.5°C initial temperature and 100 % strain	(d) for 1 Hz, 22.7°C initial temperature and 125 % strain
(e) for 0.5 Hz, 22.7°C initial temperature and 50% strain	(f) for 4.3 Hz, 22.7°C initial temperature and 50% strain	(g) for 1 Hz, 28 °C initial temperature and 50% strain	(h) for 1 Hz, 32°C initial temperature and 50% strain

3. Ramp Test

A series of ramp tests in which the VEM was subjected to a constant speed until failure were conducted at different ramp rates. Figures 7(a) and 7(b) show the shear stress and associated VEM temperature at 20%/sec and 200%/sec ramp speeds, respectively. The VEM failed at about 500% and 400% strain respectively. The failed stress was 1.7 x 10^6 Pa (250 *psi*) for 20%/sec compared to 3.4 x 10^6 Pa (500 *psi*) for 200%/sec. The failure mechanism was under strain control. It is interesting to note that the temperature rose by about 2°C for both the slow and fast strain rates. Although the VEM may be linear, it is also rate and temperature dependent, thus explaining why the stress curves were not straight lines when the VEM was subjected to a constant speed and even the temperature rise was turned off.

The model predicted reasonably well the first half of the stress time history up to about 200% strain but under-estimated the latter part since the VEM exhibited the large strain hardening effect and was highly nonlinear. Comparing the predicted stress-time curves shown in Figures 7(a)-7(b) and Figures 8(a)-8(b), it is observed that when the temperature rise was "turned off", the temperature rise slightly decreased the shear stress.

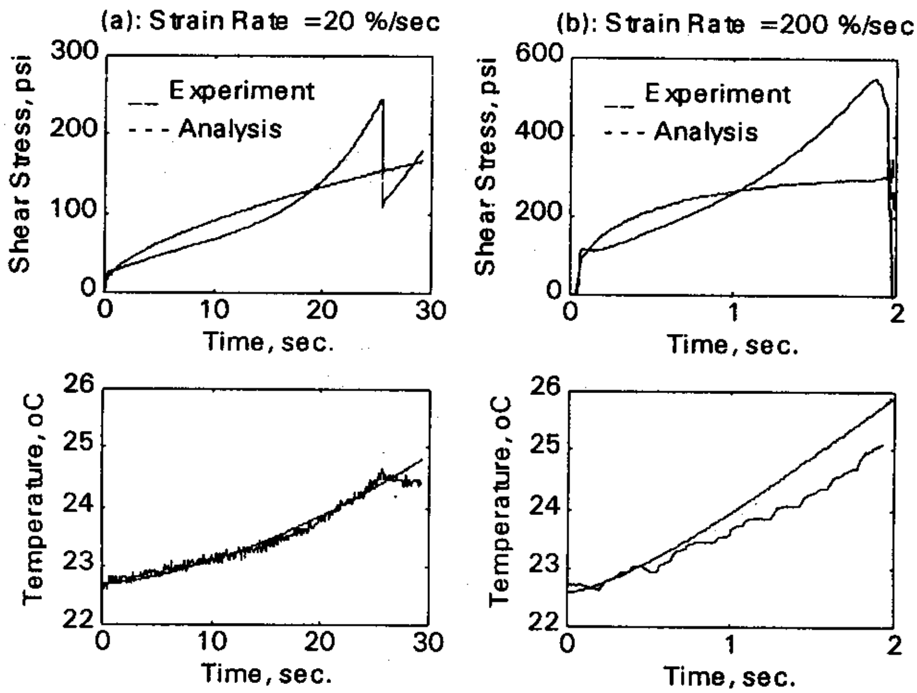

Fig. 7 Ramp tests with temperature rise consideration (1 *psi* = 6.89 kPa)

CONCLUSIONS

The study has indicated that the properties of one acrylic-based VEM, designated as 3M ISD 110, can be *essentially* linear up to 125% shear strain if the temperature rise in the VEM is artificially removed. In other words, the temperature rise appears to be the main source of non-linearity and predictable by a simple model. Any linear VEM models that work well for small strain can be modified to capture the material behavior at large strains by including the calculation of the temperature rise in the VEM. Therefore, it appears that the VEM properties can be characterized as a function of two primary parameters, *initial temperature* of VEM and *loading frequency* when the VEM specific heat and density are known. This approach has also been employed for damper design, analysis and prototype damper acceptance testing using random loading such as earthquake response (Kanitkar et al., 1998).

The constitutive VEM model used in this study has been coded as a VEM damper macro for a popular general-purpose finite analysis software package called ANSYS (Kanitkar et al., 1998). The damper macro can simply be called by the main program in the time-history analysis to represent different dampers at different times for the structural or building model without significant extra work. Computational time is doubled compared to the 'no temperature rise' case. If a damper element instead of the macro can be coded for the software, the computation should be much more efficient. In general, the peak displacement seismic response of the structure with dampers but without considering the temperature rise can be slightly under-estimated, e.g. less than 15%, compared to that with consideration of the temperature rise. The small difference between the two analyses may be attributed to the fact that the seismic response of the structure as well as damper deformation usually contains only a few large peaks. The VEM temperature rises after it did the work to dissipate the vibration energy in the structure. The total temperature rise is usually less than 10°C. Typically, dampers using 3M ISD 110 VEM are designed for a maximum shear strain of 125% or less under the maximum credible earthquake excitation. Of course, the inclusion of the temperature rise effects becomes more important when the earthquake has a long duration.

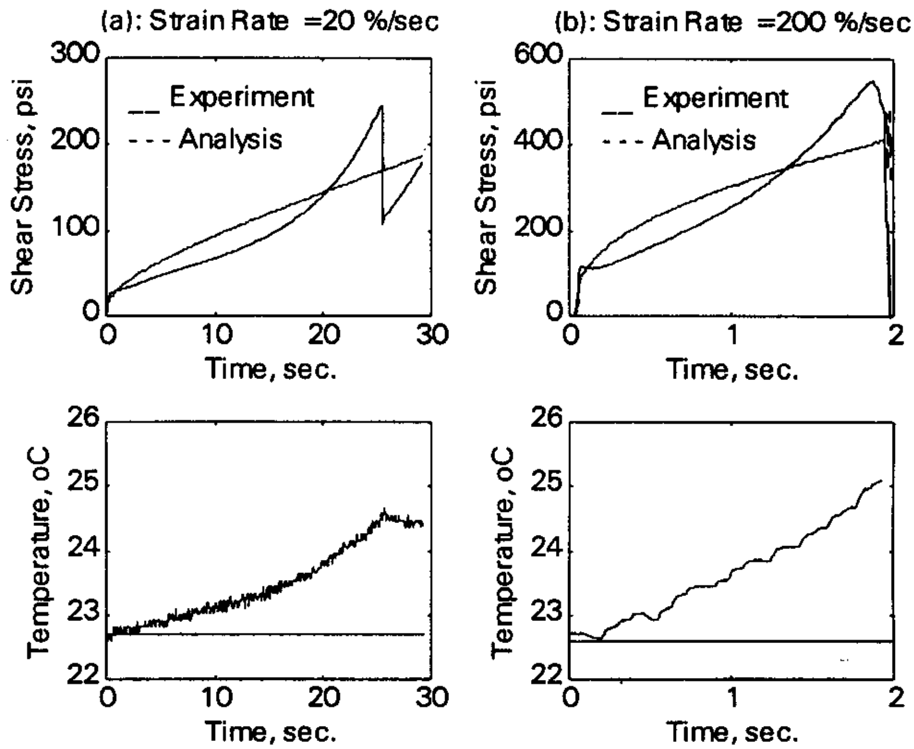

Fig. 8 Ramp tests without temperature rise consideration (1 *psi* = 6.89 kPa)

REFERENCES

1. Chang, K.C., Soong, T.T., Oh, S.-T. and Lai, M.L. (1995). "Seismic Behavior of Steel Frame with Added Viscoelastic Dampers", ASCE Journal of Structural Engineering, Vol. 121, No. 10, pp. 1418-1426.
2. Chang, K.C., Tsai, M.H., Chang, Y.H. and Lai, M.L. (1998). "Temperature Rise Effect of Viscoelastically Damped Structures under Strong Earthquake Ground Motions", 6th US National Conference on Earthquake Engineering, Seattle, WA, U.S.A.
3. Ferry, J.D. (1980). "Viscoelastic Properties of Polymers", John Wiley and Sons, Inc., New York, U.S.A.
4. Gemant, A. (1936). "A Method of Analyzing Experimental Results Obtained from Elasto-Viscous Bodies", Physics, Vol. 7, pp. 311-317.

5. Kaniktar, R., Harms, M., Lai, M.L. and Crosby, P. (1998). "Linear and Non-Linear Analysis of a Four Story Structure Using Viscoelastic Dampers", 6th US National Conference on Earthquake Engineering, Seattle, WA, U.S.A.

6. Kasai, K., Munshi, J.A., Lai, M.L. and Maison, B.F. (1993). "Viscoelastic Damper Hysteretic Model: Theory, Experiment and Application", Report ATC-17-1, San Francisco, CA, U.S.A., pp. 521-532.

7. Koh, C.J. and Kelly, J.M. (1990). "Application of Fractional Derivatives to Seismic Analysis of Base-Isolated Models", Earthquake Engineering and Structural Engineering Dynamics, Vol. 19, No. 2, pp. 229-241.

8. Lai, M.L. (1995). "Characteristics of Viscoelastic Materials and Dampers as Energy Dissipation Devices", Symposium on A New Direction in Seismic Design, Tokyo, Japan, pp. 195-210.

9. Lai, M.L. and Lunsford, D.A. (1998). "Longevity of An Acrylic-Based Viscoelastic Damper for Building Applications", 6th US National Conference on Earthquake Engineering, Seattle, WA, U.S.A.

10. Miranda, E., Alonso, J. and Lai, M.L. (1998). "Performance-Based Design of a Building in Mexico City Using Viscoelastic Dampers", 6th US National Conference on Earthquake Engineering, Seattle, WA, U.S.A.

11. Nielsen, E.J., Lai, M.L., Soong, T.T. and Kelly, J.M. (1994). "Viscoelastic Overview for Seismic and Wind Applications", SEAOC Annual Conference, California, U.S.A.

12. Shen, K.L. and Soong, T.T. (1995). "Modeling of Viscoelastic Dampers for Structural Applications", ASCE Journal of Engineering Mechanics, Vol. 121, No. 6, pp. 694-701.

13. Tsai, C.S. (1993). "Innovative Design of Viscoelastic Dampers for Seismic Mitigation", Nuclear Engineering and Design, Vol. 139, pp. 165-182.

14. Tsai, C.S. (1994). "Temperature Effect of Viscoelastic Dampers During Earthquakes", ASCE Journal of Structural Engineering, Vol. 120, No. 2, pp. 394-409.